

This article was downloaded by:

On: 21 January 2011

Access details: *Access Details: Free Access*

Publisher *Taylor & Francis*

Informa Ltd Registered in England and Wales Registered Number: 1072954 Registered office: Mortimer House, 37-41 Mortimer Street, London W1T 3JH, UK



The Journal of Adhesion

Publication details, including instructions for authors and subscription information:

<http://www.informaworld.com/smpp/title~content=t713453635>

Evaluation of the Interaction and Adsorption of γ -Glycidoxy propyl trimethoxy silane with Grit-Blasted Aluminium: A ToF-SIMS and XPS Study

Kyoko Shimizu^a; Marie-Laure Abel^a; John F. Watts^a

^a Surrey Materials Institute and Faculty of Engineering & Physical Sciences, University of Surrey, Guildford, Surrey, UK

To cite this Article Shimizu, Kyoko , Abel, Marie-Laure and Watts, John F.(2008) 'Evaluation of the Interaction and Adsorption of γ -Glycidoxy propyl trimethoxy silane with Grit-Blasted Aluminium: A ToF-SIMS and XPS Study', The Journal of Adhesion, 84: 8, 725 – 741

To link to this Article: DOI: 10.1080/00218460802352900

URL: <http://dx.doi.org/10.1080/00218460802352900>

PLEASE SCROLL DOWN FOR ARTICLE

Full terms and conditions of use: <http://www.informaworld.com/terms-and-conditions-of-access.pdf>

This article may be used for research, teaching and private study purposes. Any substantial or systematic reproduction, re-distribution, re-selling, loan or sub-licensing, systematic supply or distribution in any form to anyone is expressly forbidden.

The publisher does not give any warranty express or implied or make any representation that the contents will be complete or accurate or up to date. The accuracy of any instructions, formulae and drug doses should be independently verified with primary sources. The publisher shall not be liable for any loss, actions, claims, proceedings, demand or costs or damages whatsoever or howsoever caused arising directly or indirectly in connection with or arising out of the use of this material.

Evaluation of the Interaction and Adsorption of γ -Glycidoxy propyl trimethoxy silane with Grit-Blasted Aluminium: A ToF-SIMS and XPS Study

Kyoko Shimizu, Marie-Laure Abel, and John F. Watts

Surrey Materials Institute and Faculty of Engineering & Physical Sciences, University of Surrey, Guildford, Surrey, UK

Time-of-flight secondary ion mass spectrometry (ToF-SIMS) and X-ray photoelectron spectroscopy (XPS) have been employed to study the adsorption and interaction of γ -glycidoxy propyl trimethoxy silane (GPS) with grit-blasted aluminium.

GPS displaces adventitious hydrocarbon either by covalent bond formation between GPS and aluminium, or adsorption, when GPS is deposited on the aluminium. ToF-SIMS fragments present at a nominal mass $m/z=71$ were peak-fitted to seven peaks by using CasaXPS Software. $AlOSi^+$ and Si^+ were used to establish a relationship between covalent bond formation and the adsorption process. It is found that the adsorption isotherms of Si^+ relating to the adsorption of GPS were of the Langmuir type. The interfacial bonding between GPS and aluminium is mainly covalent at low solution concentrations. At higher concentrations (greater than $4.5 \times 10^{-4} M$) all the sites for the covalent bond formation appear to be occupied while these for the acid-base interaction are still available and then become fully occupied at solution concentrations of $4.5 \times 10^{-2} M$ and above.

Keywords: Adhesive; Aluminium; Silane; Time-of-flight secondary ion mass spectrometry; X-ray photoelectron spectroscopy

1. INTRODUCTION

The structural adhesive bonding of aluminium is carried out in many technological areas, but the most demanding, and most safety

Received 29 May 2008; in final form 25 June 2008.

One of a Collection of papers honoring John F. Watts, the recipient in February 2008 of *The Adhesion Society Award for Excellence in Adhesion Science*, Sponsored by 3M.

Address correspondence to John F. Watts, Surrey Materials Institute and Faculty of Engineering & Physical Sciences, Mail Stop A1, University of Surrey, Guildford, Surrey, GU 7XH, UK. E-mail: j.watts@surrey.ac.uk

critical, of these is certainly the use of this joining process in the aerospace industry. The structural adhesive bonding of aluminium has been shown to be a reliable and durable method of joining aluminium for aircraft manufacture and this process is used by all manufacturers worldwide. Notwithstanding the undoubted success of the procedure, the nature and quality of the pre-treatment processes is known to be a critical feature of the bonding process and the aerospace industry has developed, over the last 40 years, a variety of high quality procedures, based around acid anodizing technology, that ensures optimum performance of adhesively bonded aluminium structures. All methods currently used in the aerospace industry involve the use of Cr(VI) containing baths for either etching or anodizing purposes and there has been intensive activity in recent years to find environmentally acceptable alternatives to these potentially teratogenic solutions [1].

There is a variety of alternative processes to Cr(VI) containing pretreatments for aluminium that have been considered worthy of investigation including: chromium free anodising, Ti/Zr based processes, phosphating, plasma sprayed oxide layers, cerium based processes, organosilane treatments, self-assembled monolayers, and plasma polymerised layers [1–3]. Over the last decade, research in the authors' laboratory has led to a much improved understanding of the mode of action of organosilane adhesion promoters, both when applied as a primer layer and when incorporated into the formulation of a structural adhesive [4–8]. One critical observation, made using high spectral resolution time-of-flight secondary ion mass spectrometry (ToF-SIMS), has been the formation of a covalent bond between the organosilane molecule and the oxidised aluminium surface [9]. This is the likely source of the improved durability that has been observed by many workers when an organosilane is added as a discrete primer layer ahead of bond assembly. The covalent bond is much more resilient to hydrodynamic degradation than an interface which relies solely on secondary bonds. The primary bond, as opposed to van der Waals bonding, although not necessarily adding to the initial strength of the joint, will ensure that it exhibits good durability throughout its lifetime [6].

The aim of the current work is to examine the relationship between organosilane adsorption on a grit blasted aluminium surface with the formation of a covalent bond of the Al-O-Si type. The adsorption characteristics of a commercial organosilane adhesion promoter: γ -glycidoxy propyl trimethoxy silane (GPS), on aluminium has been studied by monitoring the uptake of GPS using ToF-SIMS and constructing liquid phase adsorption isotherms. In order to obtain a high degree of precision

of the intensity of the AlOSi^+ fragment, one of up to seven components at this mass, a curve fitting procedure has been applied to high resolution ToF-SIMS spectra at nominal mass 71 u^1 . In this manner it is possible to correlate the capacity of the solid surface for GPS with the propensity to form interfacial covalent bonds.

2. EXPERIMENTAL

2.1. Sample Preparation

Aluminium sheets (99.0% purity) were supplied by Goodfellow Cambridge Ltd. (Huntingdon, UK). These were cleaned using a Scotch-brite pad with detergent and tap water, in order to partially remove the oxide layer, followed by rinsing with acetone. The aluminium sheet was then grit-blasted with $50 \mu\text{m}$ alumina grit. Discs of 10 mm in diameter were punched from aluminium sheets and subsequently cleaned with acetone using an ultrasonic bath to remove any contamination.

GPS solutions in the range 4.5×10^{-1} to $4.5 \times 10^{-8} \text{ M}$ were prepared. Firstly, a $4.5 \times 10^{-1} \text{ M}$ of GPS was prepared by dissolving 5 ml of GPS (A-187, GE Specialty Materials, Satigny, Switzerland) in deionised water at pH 5.5 in a 50 ml volumetric flask (the density of GPS is 1.07 g/cm^3 and molecular weight is 236.34 g/mol). The pH was the natural pH of the solution. The solution was then left to hydrolyse for an hour with stirring. Subsequently, the solution was diluted to provide a set of solutions each decreasing in the concentration of GPS by an order of magnitude within a very short time. Condensation might occur at alkaline pH, longer hydrolysis time, and high GPS concentration as shown by Bertelsen and Boerio [10]; therefore, these conditions were carefully considered to prevent condensation and oligomerization during preparation.

Grit-blasted aluminium samples were dipped in 20 cm^3 of the candidate GPS solution for 10 minutes. The samples were then immediately rinsed with deionised water twice for 5 minutes, using an ultrasonic bath. Duplicate samples were prepared for XPS and ToF-SIMS analysis at each concentration.

Previous work by Abel *et al.* [11] investigated the chemisorption of GPS and found that adsorption was of the Langmuir type within a narrow range of GPS concentration, between 1 and 8% (v/v). The behaviour of adsorption at more dilute concentrations might be different so a wide range of GPS concentrations, between 4.5×10^{-8} and

¹u is unified mass unit, the IUPAC approved unit for mass spectrometry, defined as one twelfth of the mass of a ¹²C isotope in its ground state.

$4.5 \times 10^{-1} \text{ M}$ (1×10^{-6} to 10 v/v %), was used in this study to ascertain the type of adsorption over this lower concentration range.

2.2. XPS Analysis

XPS analysis was achieved using a Sigma Probe instrument (Thermo Scientific, East Grinstead, UK). The analyser was operated in the constant analyser energy (CAE) mode at a pass energy of 100 eV for survey spectra and a pass energy of 20 eV (C1s and Al2p) and 50 eV (O1s, Si2p and Na1s) for high resolution spectra of the elements of interest. Mg K α radiation with an energy of 1253.6 eV at a power of 200 W was used. The analysis area was *ca.* 500 μm in diameter. Spectral processing, quantification, and carbon peak signal peak fitting were carried out using the computer software Avantage v3.75 provided by the manufacturer of the spectrometer.

2.3. ToF-SIMS Analysis

ToF-SIMS analysis was achieved using a TOF.SIMS 5 system (ION-TOF GmbH, Münster, Germany). Static SIMS conditions with a total ion dose of less than 1×10^{13} ions cm^{-2} analysis were employed using a pulsed 8 keV Bi $_3^+$ primary ion beam. The analysis area was $100 \times 100 \mu\text{m}^2$ at a resolution of 64×64 pixels. SIMS spectra were acquired over a mass range of 0–850 u in both the positive and the negative ion modes, to provide both positive and negative static SIMS spectra.

Fragments of known composition, such as H $^+$, CH $_3^+$, Na $^+$, H $^-$, C $^-$, and CH $^-$ were used for mass calibration. In addition, characteristic aluminium and GPS fragments were also used.

The ToF-SIMS intensities for particular fragment ions under consideration were quantified using the concept of their relative peak intensity (RPI):

$$\text{RPI}_x = I_x / I_{\text{total}},$$

where x is the ion of interest and I_{total} is the total ion intensity between $m/z = 0$ and 840 u, and I_x is the measured intensity of the ion under consideration.

Peak fitting of the high resolution ToF-SIMS spectra of nominal mass 71 was carried out in order to distinguish AlOSi $^+$ from Al $_2$ OH $^+$ which are extremely close to each other, using the computer software CasaXPS provided by Casa Software Ltd. (Teignmouth, UK). To the authors' knowledge this procedure has been performed for the first time on ToF-SIMS data in this work. This procedure is not usually employed in ToF-SIMS although it is used as a standard practice in

XPS. Peak shapes were chosen to provide consistent fits across the full range of the spectra. This is easier for ToF-SIMS spectra than with XPS data as the background is much less intense. The following peak fitting parameters were used. The line-shape was a combination of 30% Lorentzian and 70% Gaussian. An asymmetry index (a) with a value of -0.2224 was used. The asymmetry index (a) is given by:

$$a = 1 - (\text{HWHM}_{\text{right}}/\text{HWHM}_{\text{left}}), \quad (1)$$

where $\text{HWHM}_{\text{right}}$ is the half width at half maximum of the right asymmetric side of peak. The value of full width at half maximum (FWHM) was used between 0.009 and 0.015 u.

3. RESULTS

3.1. XPS Analysis

Table 1 shows the surface compositions, by XPS, of the grit-blasted aluminium and samples treated with GPS. Grit-blasted aluminium exhibits a relatively high carbon concentration together with a low concentration of oxygen and aluminium, compared with samples treated with GPS. The sodium probably originates from the grit used for grit blasting [4]. The intensities of silicon gradually increase from the sample treated with the lowest concentrated GPS solution to the highest one. The silicon signal is also detected from the grit-blasted aluminium without GPS; this can originate from grit blasting processes as a silicone grease contamination such as polydimethylsiloxane (PDMS). Figure 1 presents the high resolution Si2p spectrum obtained from aluminium treated with 4.5×10^{-1} M GPS. The high

TABLE 1 XPS Surface Composition for Various Samples

Sample treatment	Surface concentration (atomic %)				
	C	Al	O	Si	Na
Grit-blasted aluminium	37.5	14.5	44.5	0.2	3.1
4.5×10^{-8} M GPS	26.8	18.3	52.8	0.5	0.6
2.3×10^{-7} M GPS	26.5	18.6	53.1	0.5	0.5
4.5×10^{-7} M GPS	26.5	18.6	53.0	0.4	0.4
2.3×10^{-6} M GPS	22.0	18.3	58.2	0.5	0.6
4.5×10^{-6} M GPS	28.7	17.7	51.5	0.5	0.5
4.5×10^{-5} M GPS	19.9	19.0	59.2	0.6	0.5
4.5×10^{-4} M GPS	23.4	19.4	55.8	0.7	0.3
4.5×10^{-2} M GPS	18.5	21.1	58.3	0.7	0.4
4.5×10^{-1} M GPS	20.2	20.4	57.1	1.0	0.4

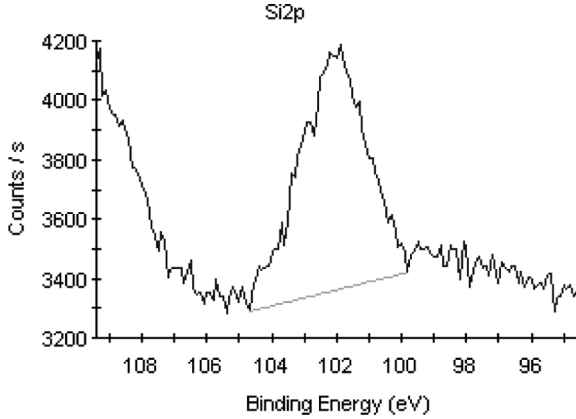


FIGURE 1 High resolution Si2p spectrum of aluminium treated with 4.5×10^{-1} MGPS.

resolution Si2p spectrum exhibits binding energy at 102 eV for all samples, and this indicates that the Si2p signal is assigned to organic rather than inorganic silicon [8].

Table 2 shows the surface concentrations for the different chemical states of carbon established by peak fitting of the C1s core level spectra. The first C1s peak at binding energy 285.0 eV is assigned to hydrocarbon, C-C/C-H. The binding energy of the second peak between 286.1 and 286.5 eV is assigned to alcohol and/or ether carbon groups, C-OH/C-O, the binding energy of the third peak is between 287.9 and 288.1 eV and is assigned to carbonyl carbon, C=O, the binding energy of the fourth peak between 289.5 and 289.9 eV is assigned to acid and ester carbon groups, O-C=O and CO_3^{2-} have binding energies at 288.9 and 289.6 eV, respectively [12,13]. As the concentration of GPS increases, signals of the first and the last peaks gradually decrease whereas signals of the second and the third peaks tend to increase slightly.

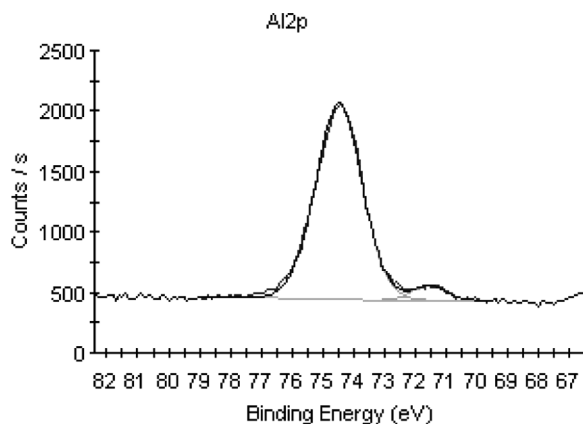
Figure 2 presents the Al2p peak fitting of the grit-blasted aluminium. The aluminium signals are peak fitted with two components: aluminium metal (Al^0) and its oxide species (Al^{3+}). The first peak at 71.1 to 71.5 eV of the binding energy is assigned to Al^0 . The second peak exhibits a binding energy shift ranging from 3.0 to 3.4 eV corresponding to Al^{3+} .

The aluminium oxide thickness can be calculated using the modified Beer-Lambert equation [14]:

$$d = \lambda_{\text{ox}} \cos \theta \ln(1 + D_m \lambda_m I_{\text{ox}} / D_{\text{ox}} \lambda_{\text{ox}} I_m), \quad (2)$$

TABLE 2 The Data of C1s Peak from all Samples, Giving the Surface Concentration and the Binding Energies of Each Component

Sample treatment	Surface concentration of C1s peak fitting (atomic %) [The binding energies of C1s peak fitting (eV)]			
	1st peak C-C/C-H	2nd peak C-OH/C-O	3rd peak C=O	4th peak O-C=O/CO ₃ ²⁻
Grit-blasted aluminium	26.8 (285.0)	4.0 (286.5)	1.1 (288.1)	5.6 (289.9)
4.5×10^{-8} M GPS	15.4 (285.0)	5.7 (286.4)	1.7 (288.0)	4.0 (289.8)
2.3×10^{-7} M GPS	16.6 (285.0)	5.0 (286.4)	1.3 (287.9)	3.6 (289.7)
4.5×10^{-7} M GPS	15.8 (285.0)	5.2 (286.4)	1.6 (287.9)	3.8 (289.7)
2.3×10^{-6} M GPS	10.9 (285.0)	5.2 (286.4)	1.6 (287.9)	4.2 (289.5)
4.5×10^{-6} M GPS	16.6 (285.0)	6.3 (286.4)	2.2 (288.0)	3.6 (289.8)
4.5×10^{-5} M GPS	8.5 (285.0)	5.5 (286.4)	2.1 (288.1)	3.7 (289.9)
4.5×10^{-4} M GPS	11.1 (285.0)	6.2 (286.4)	2.1 (288.0)	3.9 (289.8)
4.5×10^{-2} M GPS	8.4 (285.0)	5.3 (286.4)	1.8 (287.9)	3.0 (289.6)
4.5×10^{-1} M GPS	10.1 (285.0)	5.7 (286.5)	1.7 (287.9)	2.6 (289.5)

**FIGURE 2** Al₂p peak fitting of the grit-blasted aluminium.

where d is the oxide aluminium thickness, D_m and D_{ox} are the densities of the aluminium in the metal and the oxide phase, λ_m and λ_{ox} are the attenuation length of the photoelectrons in the metal and in the oxide, I_m and I_{ox} are the intensities of the aluminium and the oxide aluminium, and θ is the photoelectron take-off angle to the surface normal (Sigma Probe has a take-off angle of 53°). According to $D_m = 0.100$ moles cm^{-3} , $D_{ox} = 0.078$ moles cm^{-3} , $\lambda_{ox} = 2.4$ nm, and $\lambda_m/\lambda_{ox} = 0.79$, Equation (2) gives:

$$d = 2.4 \cos 53^\circ \ln(1 + 1.01 I_{ox}/I_m). \quad (3)$$

The thicknesses of aluminium oxide are almost constant and range between 4.2 and 5.1 nm for all samples.

3.2. ToF-SIMS Analysis

Figure 3 shows the positive and the negative ToF-SIMS spectra in the mass range of $m/z = 0$ to 300 u of the aluminium treated with 4.5×10^{-2} M GPS. The main positive and negative fragments of GPS are given in Tables 3 and 4, respectively [6,15].

In the positive mode, characteristic GPS fragments are observed at $m/z = 28, 57, 71, 79,$ and 107 and characteristic aluminium fragments are observed at $m/z = 27$ (Al^+), 61 ($\text{Al}(\text{OH})_2^+$), 103 ($\text{Al}_2\text{O}_3\text{H}^+$), 121 ($\text{Al}_2\text{O}_4\text{H}_3^+$), 163 ($\text{Al}_3\text{O}_5\text{H}_2^+$), 205 ($\text{Al}_4\text{O}_6\text{H}^+$), 223 ($\text{Al}_4\text{O}_7\text{H}_3^+$), 247 (Al_5O_7^+), and 265 ($\text{Al}_5\text{O}_8\text{H}_2^+$). PDMS fragments, as contamination, are observed at $m/z = 73$ (SiC_3H_9^+), 147 ($\text{Si}_2\text{C}_5\text{H}_{15}\text{O}^+$), and 207 ($\text{Si}_3\text{C}_5\text{H}_{15}\text{O}_3^+$). However, the amount of PDMS is small, thus, it does not affect the intensity of Si^+ much. In the negative mode, characteristic GPS fragments are observed at $m/z = 77, 121,$ and $137,$ and characteristic aluminium fragments are found at $m/z = 59$ (AlO_2^-), 77 (AlO_3H_2^-), 119 ($\text{Al}_2\text{O}_4\text{H}^-$), 137 ($\text{Al}_2\text{O}_5\text{H}_3^-$), 179 ($\text{Al}_3\text{O}_6\text{H}_2^-$), 197 ($\text{Al}_3\text{O}_7\text{H}_4^-$), 239 ($\text{Al}_4\text{O}_8\text{H}_3^-$), and 281 ($\text{Al}_5\text{O}_9\text{H}_5^-$).

In the positive mode of detection AlOSi^+ fragment, which indicates bonding between GPS and aluminium, is observed at a nominal mass of 71. However, fragment masses of AlOSi^+ and Al_2OH^+ are close to each other so peak fitting is an appropriate and convenient way to establish the intensity of AlOSi^+ fragment. Figure 4 shows the spectrum of mass 71 obtained at high mass resolution for aluminium treated with (a) 4.5×10^{-1} M GPS, (b) 4.5×10^{-1} M GPS, and (c) without GPS. The peak may be divided into seven components. Table 5 presents all masses obtained from the peak fitting for all samples with their respective assignments. Fragment masses are calculated from exact individual mass [16] according to Abel *et al.* [9]. The first peak is $^{71}\text{Ga}^+$ which originates from the aluminium substrate. The second

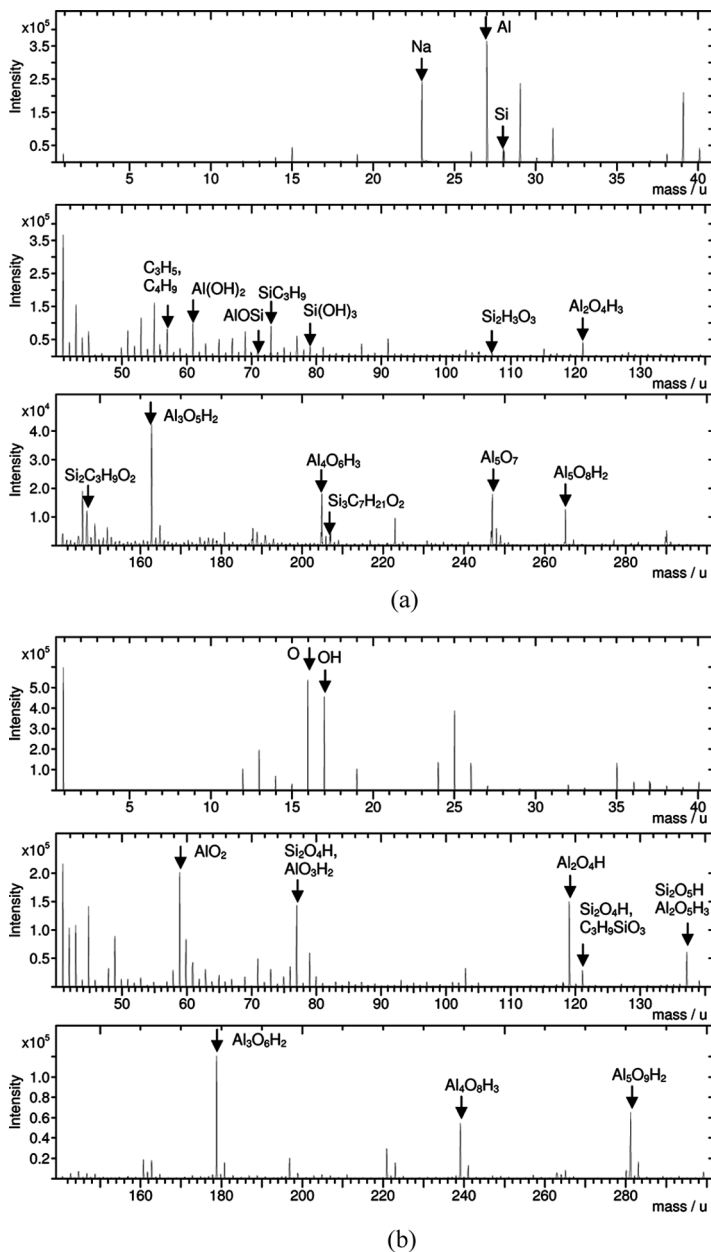


FIGURE 3 ToF-SIMS spectra for aluminium treated with 4.5×10^{-2} M GPS (a) positive (b) negative mode.

TABLE 3 Characteristic Fragments of GPS in the Positive Mode

Mass	Formula	Structure
28	Si ⁺	
45	SiOH ⁺	Si ⁺ -OH
57	C ₃ H ₅ O ⁺	$\begin{array}{c} \text{H}_2\text{C}-\text{CH}-\text{CH}_2^+ \\ \\ \text{O} \end{array}$
59	CH ₂ SiOH ⁺	H ₂ C=Si ⁺ -OH
71	AlOSi ⁺ / SiOC ₂ H ₃ ⁺ / C ₃ H ₃ O ₂ ⁺ / C ₄ H ₇ O ⁺	Al-O-Si ⁺ H ₂ C=CH-Si ⁺ =O $\begin{array}{c} \text{H}_2\text{C}-\text{CH}-\text{C}\equiv\text{O}^+ \\ \\ \text{O} \end{array}$ HC ⁺ =CH-CH ₂ -O-CH ₃
79	Si(OH) ₃ ⁺	$\begin{array}{c} \text{OH} \\ \\ \text{Si}^+-\text{OH} \\ \\ \text{OH} \end{array}$
107	Si ₂ H ₃ O ₃ ⁺	$\begin{array}{c} \text{H}-\text{Si}-\text{O}-\text{Si}^+-\text{H} \\ \quad \\ \text{O} \quad \text{OH} \end{array}$
133	C ₄ H ₁₃ OSi ₂ ⁺	$\begin{array}{c} \text{CH}_3 \quad \text{CH}_3 \\ \quad \\ \text{CH}_2 \quad \text{CH}_2 \\ \quad \\ \text{H}-\text{Si}-\text{O}-\text{Si}^+-\text{H} \\ \\ \text{H} \end{array}$

peak is AlOSi⁺, and the third peak is Al₂OH⁺. The fragment masses of the fourth peak for samples of GPS treatment are detected within the range 70.9865 and 70.9951 u, while that for the grit-blasted aluminium is 70.9862 u which is a slightly lower value than for GPS treated samples. Therefore, the fourth peak for GPS treated samples is mainly SiOC₂H₃⁺ which is a part of the GPS structure, whereas C₂HNa₂⁺ and SiOC₂H₃⁺ are for the grit-blasted aluminium. The last peak is a hydrocarbon fragment, C₅H₁₁⁺.

4. DISCUSSION

4.1. Adsorption Isotherms

In positive spectra $m/z = 28$ is the characteristic fragment of GPS (Si⁺) and $m/z = 71$ represents the covalent bond formation between aluminium and GPS (Al-O-Si⁺). Therefore, the two fragments were employed to study the relationship between surface adsorption and interaction between adsorbate and the solid surface. Table 6 shows their RPIs for nine different concentrations of GPS on the grit-blasted

TABLE 4 Characteristic Fragments of GPS in the Negative Mode

Mass	Formula	Structure
77	SiO_3H^-	$\begin{array}{c} \text{O} \\ \\ \text{Si}-\text{OH} \\ \\ \text{O}^- \end{array}$
121	$\text{C}_3\text{H}_9\text{SiO}_3^-/\text{Si}_2\text{O}_4\text{H}^-$	$\begin{array}{c} \text{OH} \\ \\ \text{CH}_3-\text{CH}_2-\text{CH}_2-\text{Si}-\text{OH} \\ \\ \text{O}^- \\ \\ \text{H} \quad \text{O}^- \\ \quad \\ \text{Si}-\text{O}-\text{Si} \\ \quad \\ \text{O} \quad \text{O} \end{array}$
137	$\text{Si}_2\text{O}_5\text{H}^-$	$\begin{array}{c} \text{OH} \quad \text{O}^- \\ \quad \\ \text{Si}-\text{O}-\text{Si} \\ \quad \\ \text{O} \quad \text{O} \end{array}$

aluminium and the grit-blasted only aluminium which is used as a reference. As a general trend, the RPIs of Si^+ and AlOSi^+ fragments increase when the concentration of GPS is increased.

The adsorption and the covalent bond formation curves are constructed by plotting their RPIs against the concentration of GPS, as shown in Figure 5. The uptake increases very quickly at highly dilute solution concentration, and reaches a plateau. This behaviour shows typical chemisorption and indicates that all the potential adsorption sites on the substrate are occupied by adsorbate molecules [17]. The type of adsorption isotherm is tested by using Langmuir, Temkin, and Freundlich equations for which the theory is described elsewhere [18–20], and the least square values (R^2) are 0.99, 0.72, and 0.78, respectively. The R^2 value for the Langmuir plot is closer to 1 than the other two types of plot; thus, it is confirmed that the uptake of GPS on grit-blasted aluminium is of the Langmuir type monolayer coverage.

4.2. Behaviour of GPS on the Aluminium Substrate

When GPS deposits on the aluminium surface, GPS interacts by formation of a covalent Al-O-Si bond *via* condensation between hydroxyls present at the aluminium surface and silanols of the hydrolysed silane

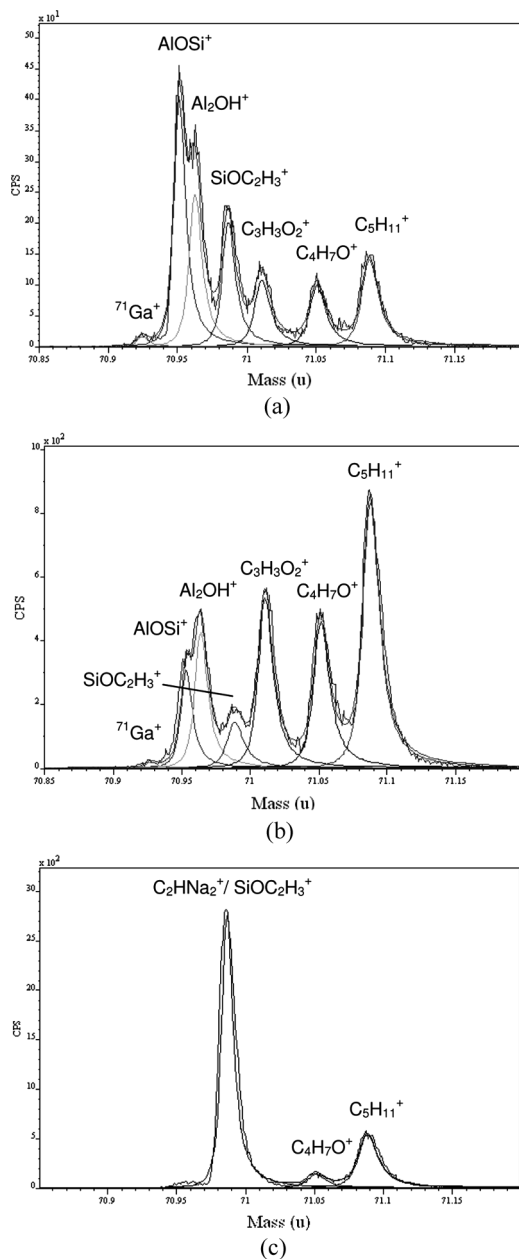
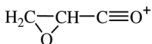


FIGURE 4 Spectrum at high resolution of aluminium treated with (a) 4.5×10^{-1} M GPS, (b) 4.5×10^{-6} M GPS, and (c) without GPS for nominal mass $m/z = 71$.

TABLE 5 Fragments Obtained at Nominal Mass 71 and Their Respective Assignments for Aluminium Treated GPS

Peak no.	Experiment mass (m/z)	Exact mass (m/z)	Formula	Structure
1	70.9230–70.9287	70.9247	$^{71}\text{Ga}^+$	
2	70.9510–70.9530	70.9534	AlOSi^+	$\text{Al}-\text{O}-\text{Si}^+$
3	70.9621–70.9650	70.9658	Al_2OH^+	$\text{Al}^+=\text{Al}-\text{OH}$
4	70.9862–70.9951	70.9874	C_2HNa_2^+	$\text{Na}-\text{C}^+=\text{CH}-\text{Na}$
		70.9953	$\text{SiOC}_2\text{H}_3^+$	$\text{H}_2\text{C}=\text{CH}^+=\text{Si}=\text{O}$
5	71.0104–71.0122	71.0133	$\text{C}_3\text{H}_3\text{O}_2^+$	
6	71.0504–71.0519	71.0497	$\text{C}_4\text{H}_7\text{O}^+$	$\text{HC}^+=\text{CH}-\text{CH}_2-\text{O}-\text{CH}_3$
7	71.0867–71.0882	71.0861	$\text{C}_5\text{H}_{11}^+$	$\text{CH}_3-\text{CH}_2-\text{CH}_2-\text{CH}_2-\text{CH}_2^+$

[9]. Besides, the epoxy group from the end of the GPS molecule can also adsorb on aluminium surface as shown by Woods *et al.* using reflection-absorption infrared spectroscopy (RAIRS) [21], and this adsorption is an acid-base type of interaction, as shown in Figure 6.

The thicknesses of aluminium oxide are almost constant for all samples. However, the full width at half maximum (FWHM) value of

TABLE 6 Relative Intensity of Characteristic Positive and Negative Ions of Samples

Sample treatment	Relative Peak Intensity ($\times 10^5$)	
	Positive m/z = 28 u	Positive m/z = 71 u
Grit-blasted aluminium	1.9	–
4.5×10^{-8} M GPS	10.1	4.4
2.3×10^{-7} M GPS	13.8	5.9
4.5×10^{-7} M GPS	10.9	4.2
2.3×10^{-6} M GPS	17.9	5.8
4.5×10^{-6} M GPS	15.6	5.9
4.5×10^{-5} M GPS	15.9	6.6
4.5×10^{-4} M GPS	21.3	9.3
4.5×10^{-2} M GPS	23.4	10.7
4.5×10^{-1} M GPS	42.9	12.3

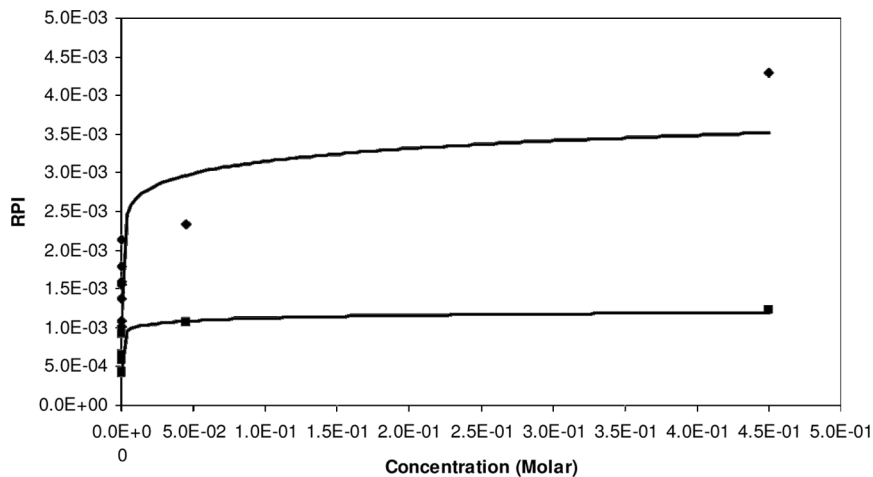


FIGURE 5 The ToF-SIMS uptake and covalent formation curves of GPS on grit-blasted aluminium, using the fragments at mass 28 (◆) and 71 (■) in positive spectra.

the aluminium oxide component for the GPS treated aluminium (2.1 eV) is wider than for the grit-blasted aluminium (1.8 eV). This is probably a result of the presence of a weak Al-O-Si component in the case of the GPS treated aluminium [22], the main Al2p contribution being from oxide and hydroxide species, the latter been slightly

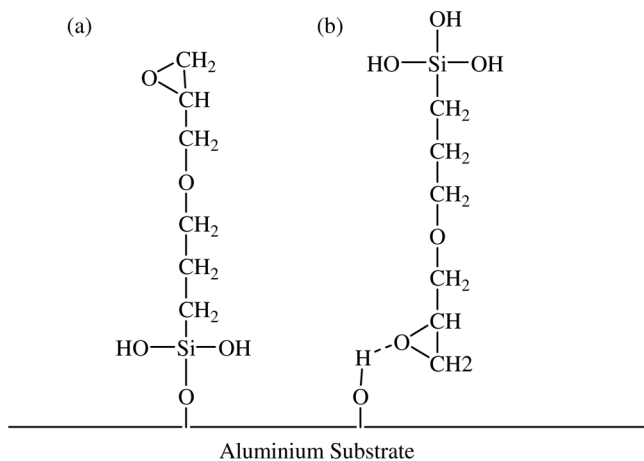


FIGURE 6 (a) Interaction and (b) adsorption of GPS with aluminium substrate.

more intense compared with the grit blasted sample, as a result of water exposure. The Si2p binding energy is also consistent with the formation of a covalent bond between organosilane and substrate as described by Helbert and Saha [23].

From the Si XPS signal, it can be seen that more GPS adsorbs on aluminium at high concentration than at low concentration. The intensity of C1s tends to decrease from low to high concentration of GPS, and the proportion of C-C/C-H also decreases as shown in Tables 1 and 2. However, the intensities of C-OH/C-O and C=O slightly increase. The hydrocarbon components originate from GPS and adventitious organic materials, although the majority of adventitious carbon is removed by washing with acetone. In addition, the oxygen bonded carbon components come from GPS and also ambient atmosphere. The small increase of C-O/C-OH might result from the increased amount of GPS. The intensity of O-C=O/CO₃²⁻ in Table 2 generally decreases as GPS solution concentration increases. This is probably due to a decrease of sodium carbonate and/or bicarbonate.

GPS includes C-C/C-H and C-O bonding while the adventitious materials mainly consist of C-C/C-H bonding. When GPS interacts with the aluminium substrate by either a formation of Al-O-Si (a covalent bond) or by an acid-base interaction, it replaces hydrocarbon which is bound through weaker van der Waals forces as shown by the decrease in intensities of the first carbon components. The adsorption of GPS is a chemisorption which forms a monolayer on the aluminium substrate, whereas adventitious carbon is a physisorption which may form multilayers. Therefore, the results indicate that GPS molecules adsorb or interact on the aluminium surface, then replace adventitious hydrocarbon, consistent with the observation that the uptake of GPS onto aluminium substrates can be described by a Langmuir isotherm. The relationship between the adsorption and the interaction of GPS on the aluminium substrate is discussed using analysis of the ToF-SIMS data.

Figure 7 shows the relationship between RPIs of Si⁺ and SiOAl⁺ fragments. When the intensity of Si⁺ fragments increases, that of SiOAl⁺ also tends to increase linearly from 4.5×10^{-8} to 4.5×10^{-2} M GPS solution concentrations. The amount of Si⁺ is related to all adsorption occurring on the substrate, whereas the amount of SiOAl⁺ illustrates directly the formation of covalent bonding. At the highest concentration, the correlation between the two fragments is lost, indicating that adsorption is of more consequence than covalent bond formation. Besides, the Si⁺ fragment can also be yielded by the SiOAl bond. Therefore, when the RPIs of Si⁺ and of SiOAl⁺ have a

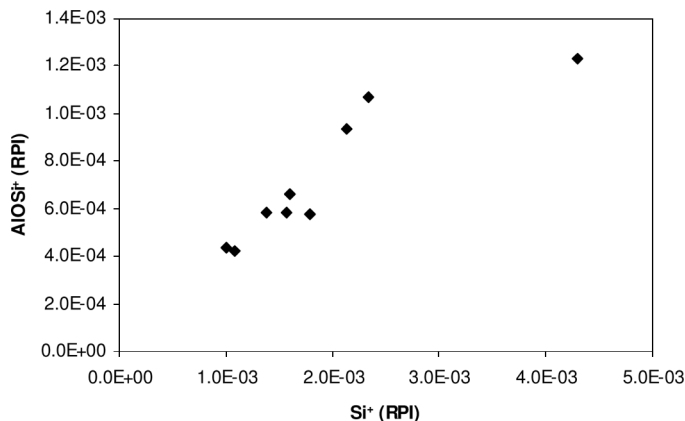


FIGURE 7 Relationship between RPI of Si⁺ and AlOSi⁺ fragment.

linear correlation below 4.5×10^{-2} M there are two possibilities: either GPS adsorption and Si-O-Al interaction have similar behaviour so they appear to be correlated, or Si-O-Al interaction is largely dominant with a true correlation. At lower concentrations there are enough sites on the aluminium oxide surface to displace the adventitious hydrocarbon (present through van der Waals bonding) to GPS (occurring through covalent bonding or acid-base interactions), and then the sites for the covalent bond are occupied at higher concentrations (greater than 4.5×10^{-4} M). The sites for the acid-base interaction are, however, still available at this concentration and they are occupied above solution concentrations of 4.5×10^{-2} M.

5. CONCLUSIONS

A study of the interaction and adsorption of GPS with grit-blasted aluminium has been carried out using XPS and ToF-SIMS including high mass resolution ToF-SIMS. The RPI of SiOAl⁺ fragment (the covalent bonding between GPS and aluminium) is obtained by peak fitting of ToF-SIMS high resolution spectra, and that of the Si⁺ fragment (the adsorption of GPS) is also obtained to study the relationship between interaction and adsorption of GPS.

The adsorption of GPS is chemisorption and the uptake isotherm is of the Langmuir type. As GPS deposits on the aluminium surface, GPS displaces adventitious carbon *via* the formation of covalent bonding and adsorption of GPS. At first, the amount of formation of covalent bonding reaches a plateau at high solution concentrations (greater than 4.5×10^{-4} M); subsequently, the adsorption of GPS reaches a

plateau above 4.5×10^{-2} M and forms monolayer of GPS on the aluminium surface.

ACKNOWLEDGMENTS

The authors are grateful to both the referees and the Editor in Chief of this journal for the extremely rapid processing of this paper. MLA thanks The Royal Society for a University Research Fellowship.

REFERENCES

- [1] Twite, R. L. and Bierwagen, G. P., *Prog. Org. Coat.* **33**, 91–100 (1998).
- [2] Kendig, M. W. and Buchheit, R. G., *Corros.* **59**, 379–400 (2003).
- [3] Kinloch, A. J., *Adhesion and Adhesives*, (Chapman and Hall, London and New York, 1995), pp. 148–165.
- [4] Rattana, A., Hermes, J. H., Abel, M.-L., and Watts, J. F., *Int. J. Adhes. Adhes.* **22**, 205–218 (2002).
- [5] Watts, J. F., Rattana, A., and Abel, M.-L., *Surf. Interf. Anal.* **36**, 1449–1468 (2004).
- [6] Rattana, A., Abel, M.-L., and Watts, J. F., *J. Adhes.* **81**, 963–988 (2005).
- [7] Rattana, A., Abel, M.-L., and Watts, J. F., *Int. J. Adhes. Adhes.* **26**, 28–39 (2006).
- [8] Sautrot, M., Abel, M.-L., and Watts, J. F., *J. Adhes.* **81**, 163–187 (2005).
- [9] Abel, M.-L., Digby, R. P., Fletcher, I. W., and Watts, J. F., *Surf. Interf. Anal.* **29**, 115–125 (2000).
- [10] Bertelsen, C. M. and Boerio, F. J., *Prog. Org. Coat.* **41**, 239–246 (2001).
- [11] Abel, M.-L., Joannic, R., Fayos, M., Lafontaine, E., Shaw, S. J., and Watts, J. F., *Int. J. Adhes. Adhes.* **26**, 16–27 (2006).
- [12] Vickerman, J. C., *Surface Analysis – The Principal Techniques*, (John Wiley and Sons, New York, 1998), pp. 50–52.
- [13] Wanger, C. D., Riggs, W. M., Davis, L. E., Moulder, J. F., and Muilenberg, G. E., *Handbook of X-ray Photoelectron Spectroscopy*, (Perkin-Elmer Corporation, Eden Prairie, MN 1979), pp. 216–217.
- [14] Olefjord, I., Mathieu, H. J., and Marcus, P., *Surf. Interf. Anal.* **15**, 681–692 (1990).
- [15] Abel, M.-L., Watts, J. F., and Digby, R. P., *Int. J. Adhes. Adhes.* **18**, 179–192 (1998).
- [16] IUPAC Commission on Atomic Weights, *Pure Appl. Chem.* **56**, 653 (1984).
- [17] Possart, W., *Adhesion – Current Research and Application*, (Wiley-VCH Verlag GmbH & Co, KGaA, Weinheim, Germany 2005), pp. 3–5.
- [18] Watts, J. F. and Castle, J. E., *Int. J. Adhes. Adhes.* **19**, 435–443 (1999).
- [19] Aeimbu, A., Castle, J. E., and Singjai, P., *Surf. Interf. Anal.* **37**, 1127–1136 (2005).
- [20] Mall, I. D., Srivastava, V. C., and Agarwal, N. K., *J. Hazard. Mater.* **143**, 386–395 (2007).
- [21] Woods, G. A., Haq, S., Richardson, N. V., Shaw, S., Digby, R., and Raval, R., *Surf. Sci.* **433–435**, 199–204 (1999).
- [22] Franquet, A., Biesemans, M., Terryn, H., Willem, R., and Vereecken, J., *Surf. Interf. Anal.* **38**, 172–175 (2006).
- [23] Helbert, J. N. and Saha, N., *J. Adhes. Sci. Technol.* **5**, 905–925 (1991).